Shape Memory Polymer Research

Patrick T. Mather,[1,2] Xiaofan Luo,[1,2] and Ingrid A. Rousseau[3]

[1]Syracuse Biomaterials Institute, [2]Biomedical and Chemical Engineering, Syracuse University, Syracuse, New York 13244; email: ptmather@syr.edu, xluo06@syr.edu

[3]General Motors Corporation, R&D Center, Warren, Michigan 48090; email: ingrid.rousseau@gm.com

Annu. Rev. Mater. Res. 2009. 39:445–71

The *Annual Review of Materials Research* is online at matsci.annualreviews.org

This article's doi: 10.1146/annurev-matsci-082908-145419

1531-7331/09/0804-0445$20.00

Key Words

shape memory polymers, networks, thermomechanical properties, smart materials

Abstract

The past several years have witnessed significant advances in the field of shape memory polymers (SMPs) with the elucidation of new compositions for property tuning, the discovery of new mechanisms for shape fixing and recovery, and the initiation of phenomenological modeling. We critically review research findings on new shape memory polymers along these lines, emphasizing exciting progress in the areas of composites, novel recovery triggering, and new application developments.

BASIC PRINCIPLES OF SHAPE MEMORY POLYMERS

Shape memory polymers (SMPs) are a class of smart materials that offer mechanical action triggered by an external stimulus. More specifically, SMPs are able to "remember" one or more shapes, each determined by network elasticity, but can be stored in temporary shapes by material immobilization, commonly by vitrification or crystallization. As a simple example, a complex three-dimensional SMP shape can be compacted into a slender form (suitable for catheter delivery to the body or to fit into an otherwise compact space) by a cycle of heating, deforming, cooling, and unloading. Later, application of heat, light, or solvent exposure can trigger a return to the equilibrium, complex shape through network chain mobilization. At first glance, those familiar with polymer physics will immediately recognize the potential of many—if not most—polymeric materials to exhibit such a shape memory (SM) effect. However, what lies beneath the surface of this deceivingly simple SM cycle is a plethora of polymer chemistry and physics that seeks to test our understanding of structure-property relations and our capacity to tune properties at will. Several excellent reviews (1–7) have appeared on this topic, ranging from broadly scoped (1) to focused views on structure-property relationships (2) to medical applications (5) and finally application-specific molecular, structural, and geometrical design for optimization of SMPs (7). Herein, we present and critically address the multitude of significant developments that have recently occurred in the field of SMP research during the past several years, revealing significant innovations and scientific progress. We hope to show that research in the field of SMP materials is quite active, innovative, and expanding into a large number of application areas that exploit their unique properties.

We begin with a description of the principal SM cycle. The evolution of stress (or force), strain, and temperature during thermomechanical cycling of an SMP is referred to as the SM cycle. It can be plotted as shown in **Figure 1** for cross-linked poly(cyclooctene) (8), a semicrystalline network polymer. Initially, at a temperature (T_d) higher than the SMP transition temperature (T_{trans}), at which the material exists in a rubbery, elastic state, the material is deformed to a certain strain. Subsequent cooling under constant stress (or strain) to a temperature (T_f or $T_s < T_{\text{trans}}$) causes the material to adopt a more rigid state, in this case the semicrystalline state, therein immobilizing the constituent polymer chains and allowing fixing or freezing of the deformation as latent strain energy. Therefore, upon unloading at T_f, a minor instantaneous recovery may occur. The shape recovery is achieved by heating the material without any stress (unconstrained) to a temperature generally greater than T_{trans}. The stored strain energy is then released owing to the regained chain mobility. The primary driving force for shape recovery is entropic in nature; it is energetically favorable for the material to return to its most disordered conformation.

The abilities of SMPs to fix a temporary shape and to recover an original shape in a controlled fashion through use of external stimuli (i.e., heat, electric field, magnetic field, irradiation) distinguish them from most conventional polymeric materials. Shape fixing and shape recovery reflect the various microstructural transformations and determine the extent to which SMPs can be practically used, and are, therefore, of both fundamental and practical importance. Clearly a variety of figures of merit, including the quality of fixing and recovery, can be conceived in addition to the sharpness of the recovery event and the work capacity, among others. These are discussed throughout our review.

Shape fixing, or fixity, refers to the ability of an SMP to retain a temporary state, and thus store strain energy, by cooling below a transformation temperature. Thermodynamically, shape fixing results from a transition between a state in which changes in conformational entropy are dominant (entropic rubber) and a state with limited chain mobility. Shape fixing can be quantified by use of the measure, $R_f(\%) = \varepsilon_u/\varepsilon_m \cdot 100$, where ε_u represents the strain after unloading, ε_m is the temporal

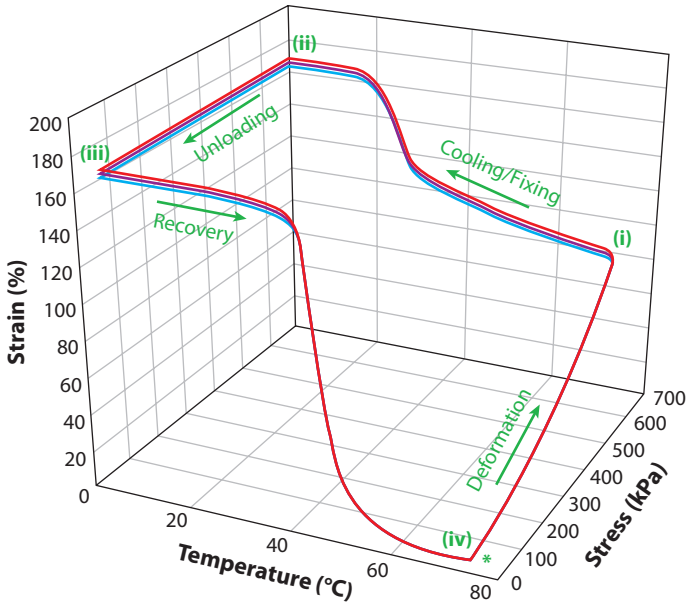

Figure 1

Thermomechanical cycles for an example of a shape memory polymer (SMP), cross-linked poly(cyclooctene). A heated, unloaded sample (*asterisk*) is deformed to state i and cooled through a fixing temperature to state ii, followed by unloading (revealing the degree of strain fixing) to state iii, and finally by unloading to the original state (*iv*) if the strain recovery is complete. Three consecutive cycles are shown, revealing excellent repeatability. Redrawn with permission from Reference 8.

strain achieved after deformation, and R_f may depend on the SM cycle number, N. At the molecular level, fixing can be designed into a SMP by designing the constituent chains to crystallize or vitrify at a targeted temperature or otherwise immobilize the chains, for example, by the establishment of a secondary and labile cross-linked network. The permanent, "memorized" shape of a SMP can be recovered from its temporarily fixed shape by applying a specific stimulus. The recovery, i.e., the stress/strain evolution over time and temperature, is of primary importance in the studies of SMPs. Free recovery—that is, recovery at no mechanical load—is the most commonly employed method to characterize shape recovery. In this manner, various measures of recovery have been described. The most common measure employed is $R_r(\%) = (\varepsilon_u - \varepsilon_p)/(\varepsilon_m - \varepsilon_p) \cdot 100$, where ε_u, ε_p, and ε_m represent the fixed strain after unloading, the permanent strain after heat-induced recovery, and the temporal strain achieved by deformation, respectively. Other figures of merit that include the SM fill factor (2) and the shape recovery sharpness (9) complement R_f with measures of the sharpness or rate of the recovery event.

NEW MATERIALS AND SHAPE MEMORY BEHAVIOR

Shape memory polyurethanes (SMPUs) remain one of the main classes of SMPs studied. Their attractiveness mainly lies in their ease of processing and low cost. Ratna & Karger-Kocsis (6) recently reviewed current advances in terms of the chemical structure/composition of SMPUs. These researchers found that optimized SM effects were obtained at a hard-segment content of 35 to 40 wt% for glassy thermoplastic SMPUs and at a soft-segment molecular weight of 5000–6000 g mol^{-1} for semicrystalline SMPUs. In addition, the importance of molecular

design was highlighted. The authors reported that the incorporation of rigid aromatic structures and/or of more planar molecules supported higher SM performances owing to stronger molecular interactions.

More recent studies aimed at counteracting some of the intrinsic disadvantages of SMPUs such as their low thermal conductivity, lower mechanical properties, and reduction in SM performance over the first several thermomechanical cycles and high-thermal-expansion coefficients. Generally, thermal conductivity is enhanced by adding conductive inorganic fillers to the polymer matrix. Recently, Razzaq & Frormann (10) used aluminum nitride (AlN) particles to improve the thermal conductivity of their commercial SMPU. At a 40 wt% loading of AlN, the authors measured an increase in thermal conductivity from 0.12 to 0.44 W $(K \cdot m)^{-1}$. Unfortunately, the inclusion of AlN also led to a large decrease in the shape recovery from 97% to 70%. Although slightly improved, the shape fixity remained low, at 45%. Ratna & Karger-Kocsis (6) reviewed other examples of inorganic fillers that have been used to increase the thermal conductivity of SMPs. Such inorganic fillers include glass fibers, Kevlar fibers, and SiC particles. Other groups have attempted to use carbon nanotubes (CNTs) for improving the thermal conductivity of their SMPUs, with only limited success. However, the incorporation of CNTs was proven useful for enhancing the mechanical properties of the pristine polymer (11, 12) as well as for widening the range of alternate SM-triggering mechanisms such as electric current (12).

By improving the mechanical properties of SMPs, researchers aim to increase the recovery forces of their materials. Meng & Hu (11) described the benefit of reinforcing their SMPU fibers with multiwall carbon nanotubes (MWNTs). By varying the loading of MWNTs from 1 to 3 wt%, they witnessed an increase in shape recovery ($R_r > 80\%$) as well as in recovery stresses from 0.12 to 0.27 cN $dtex^{-1}$ at the expense of a slight reduction in shape fixity ($R_f \sim 80\%$) compared with the pristine SMPU fibers. In contrast, they showed that a higher percentage of MWNTs rendered fiber processing difficult, which led to decreased physical properties of the fibers and hence to a degradation of their SM properties. Other studies have used alternate routes to improve the mechanical properties of their SMPUs. Xu et al. (13) synthesized a hybrid diol containing hydrolyzable Si-OEt groups as a cross-linker. The creation of covalent cross-linking in addition to the inorganic nature of the resulting Si-O-Si bonds provided these researchers' materials with increased modulus, especially above T_g, where E' increased from 3.85 to 16.34 MPa. The shape recovery was increased as well. Moreover, the authors claimed stability of the SM properties over the initial 50 thermomechanical cycles.

Because the thermal expansion coefficients of polymers are generally one to two orders of magnitude larger than those of SM alloys and SM ceramics (14), their effect (usually considered negative) on the SM behavior may become non-negligible. One way to reduce the thermal expansion is to incorporate inorganic fillers into the SMP matrix. Gunes et al. (14) evaluated the abilities of four different inorganic fillers in lowering the coefficient of linear thermal expansion (CTLE) of a chemically cross-linked semicrystalline SMPU. They found that the addition of nanosized fillers was more efficient at decreasing the CLTE. In addition, high-aspect-ratio fillers such as organoclay and carbon nanofibers (CNFs) performed better than spherical fillers. However, care must be taken because inorganic fillers having a strong interaction with the matrix polymer may disturb its crystallization behavior, hence resulting in reduced SM performance.

Because SMPs exhibit physical properties similar to those of human tissues, they are thought of as ideal candidates for many medical applications, a topic we discuss in detail below. Although many SMPUs offer biocompatibility, many groups are attempting to develop new SM materials that offer a combination of the following characteristics: biocompatibility, bioresorbability, biodegradability, and low cytotoxicity, among others. In one study, Pierce and coworkers (15) reported on a thermoplastic poly(ester urethane) that incorporated novel, in-house-synthesized,

amorphous oligomeric diols based on aliphatic diols and aliphatic diacids or substituted anhydride as soft segments. In addition to exhibiting low cytotoxicity, their new poly(ester urethane)s showed an extraordinary high elongation at break of 2106%.

Biodegradable SMPUs have been developed by Knight et al. (16), who reported on POSS (polyhedral oligosilsesquioxane)-based biodegradable SMPs exhibiting a well-defined T_g for poly(D,L-lactide) soft segments and hard segments containing the POSS moiety. Excellent phase separation was observed with a sharp soft-segment T_g largely independent of POSS loading in the hard-segment phase. Also observed was an increase in latent heat of melting of the hard-segment phase from 0.35 to 1.5 J g^{-1} with increasing POSS loading at a relatively constant T_m of 115°C. Consequently, the rubber elastic plateau increased in flatness and breadth with POSS hard-block content. The SM performances included near-perfect fixing (>99%) and strain recovery that increased with each cycle: 71%, 89%, and 93% for the first through third cycles for a tensile strain of 30%. The materials were proven to be biodegradable, opening the potential for resorbable medical implants with SM characteristics.

Recognizing the importance of good phase separation for high-quality strain fixing in thermoplastic polyurethanes, Chen et al. (17) studied the addition of low-molecular-weight additives and end-cappers to common polyester diol-based thermoplastic polyurethanes (TPUs), including those based on poly(1,4-butylene adipate) and poly(hexamethylene adipate). Strain fixing improved by 20% upon end-capping such TPUs with octadecanol (HO-$C_{18}H_{37}$). Employing a different approach to the same end, Meng & Hu (18) and Ji et al. (19) studied the impact of heat treating SMP fibers of poly(ϵ-caprolactone) (PCL)-based and poly(ethylene adipate)-based polyurethanes, respectively. In both cases, significant improvements in fixing but small impacts on recovery were witnessed. Future work should involve similar studies on polyurethanes with substantially lower hard-segment contents because this will engender higher elasticity and concomitant elastic strain fixing and recovery. We expect that improvements in SMP textiles will lead to diverse applications ranging from wound care to fabrics.

Poly(lactic acid) (PLA)-based systems exhibit SM behavior in addition to being biocompatible, biodegradable, and bioresorbable. Aiming at increasing the inertness of PLA-SMPs to the human metabolic processes, Zini & Scandola (20) developed a novel synthesis method for PLA-SMPs that uses a zirconium complex as the initiator instead of the common but more toxic stannous complex. To increase the SM properties of their PLA-SMPs, Zhou et al. (21) incorporated hydroxyhapatite (HA) particles into their synthesis. They claimed that the hydrogen bonding taking place between the PLA chains and the HA particles was responsible for the higher shape recovery (≥98% compared with 80.5% for the pristine PLA). In this case, the H bonds constituted the physical cross-links of the permanent (equilibrium) shape of the SMP, whereas the crystallization of the PLA chains was the basis of its reversible phase. Similar reinforcement strategies have been used with other polymer matrices. For instance, Zhang et al. (22) described the synthesis of poly(ethylene glycol) (PEG)-based SMPs incorporated with PEG-α-cyclodextrin of varying polarities and hydrophilicities. At 60% loading, shape recovery increased to 97%. The authors observed that the higher the ratio of storage moduli below and above T_g (E'_g/E'_r), the better the shape fixing and the shape recovery were. Interestingly, two of their formulations showed high modulus at approximately plateau 1 GPa. These values could translate to extremely high recovery stresses, although this property was not evaluated in this study, compared with commonly reported values.

Another group has worked on biodegradable poly(L-lactide) (PLLA) (23) prepared by ring-opening polymerization of L-lactide monomer. Modest SM behavior was observed for films tested in bending, with 8% bending allowing near-100% recovery but 20% bending showing a reduced recovery of 70% and recovery decreasing with each cycle. Elasticity above T_g was likely

compromised by the high level of crystallinity typical of PLLA materials. Thus, deformations being fixed for subsequent recovery likely featured a significant plastic component related to a crystalline phase rearrangement that was unrecoverable upon heating.

For semicrystalline thermoplastics to exhibit the elasticity necessary for desirable SM, an optimally low level of crystallinity is required. As an approach to achieving optimal crystallinity in poly(L-lactide), Lu et al. (24) copolymerized L-lactide with varying levels of ϵ-caprolactone (CL), up to 40%. The samples prepared in the range of 0 to 30 mol% CL showed decreased crystallinity from 29% to 8.7%, with T_m and T_g decreasing from 174°C to 125°C and from 62°C to 25°C, respectively. Crystallinity was lost completely for 40% CL. Shape recovery increased monotonically from 65% to 99% over the range of 0 to 40 wt% CL. That the recovery was high for the amorphous sample (40%) suggests that the elasticity is derived from entanglements in that particular sample. T_m-based SM was witnessed for another biodegradable polymer: microbe-synthesized poly(3-hydroxy butyrate)-*co*(3-hydroxy valerate) (PHBV) polymer prepared with a uniquely high 3-hydroxy-valerate content (35%) by use of the *Pseudomonas* sp. *HJ-2* organism (25). In a manner similar to strain-induced crystallization of synthetic polyurethanes for SM (26), the PHBV polymer demonstrated strain fixing at a temperature below or within the complex melting transition. The measured strain recovery was quite complete and ostensibly derived from entanglements. Because PHBV materials are well established as biocompatible and biodegradable polymers (27), exploitation of the SM effect of the type shown by Kim et al. (25) for medical applications is likely. However, the very broad and complex melting behavior of this natural polymer, which renders the fixing relatively poor, presents challenges to actual utilization in medical devices.

New thermosetting and biodegradable T_g-based SMPs were conceived and studied by Alteheld and coworkers (28) to feature star-shaped PLGA triols and tetra-ols (four-arm stars) cross-linked with aliphatic diisocyanates. Variation in network composition allowed for the systematic variation in T_g over the range of 48°C to 66°C. This work built upon prior work from the same group on semicrystalline networks that incorporated PCL dimethacrylates as cross-linker copolymerized with a low-T_g-forming butyl acrylate comonomer (29). In the newer, PLGA-based networks, a combination of good properties was achieved: optical transparency, good strain fixing ($R_f \sim 95\%$), near-complete recovery ($R_r > 98\%$), and relatively fast degradation kinetics compared with PCL networks. Although the strain fixing and recovery in the new materials were excellent, the very broad recovery events—as large as 40°C—may hamper the ability to use such materials in medical applications for which a restrictive operating window of 40°C to 50°C exists.

Along similar lines, Kelch et al. (9) prepared conetworks of PLGA-dimethacrylate and two alkyl acrylates, with an aim at achieving an elastomeric yet T_g-based SMP akin to the SMPs of Rousseau & Mather (30). (Ordinarily, T_g-based SMPs feature glassy tensile moduli in excess of 1 GPa.) As such, Kelch et al. (9) sought an interpenetrating network structure of PLGA glass and alkyl acrylate elastomer, which was achievable for compositions incorporating the hexyl acrylate monomer. Tensile moduli in the range of 10 to 300 MPa were achieved, and good SM characteristics of fixing and recovery were observed. A useful measure of shape recovery sharpness was utilized: $v_r = R_r/\Delta T$, where ΔT is the temperature window of recovery so that large values of v_r indicate sharper recovery events. For the materials studied, this figure of merit ranged from 1.8% $°C^{-1}$ to 4.2% $°C^{-1}$.

Recent studies performed by Yakacki et al. (31, 32) aimed at developing acrylates-SMPs as potential candidates for biomedical applications. The authors described the cross-linking reaction of *t*-butyl acrylate with poly(ethylene glycol dimethacrylate). Increasing the cross-linker amount from 10% to 40% led to SMPs with T_g ranging from 48°C to 52°C, rubbery moduli increasing from 1.2 to 8.5 MPa, and decreasing strain-to-failure. As is discussed in more detail below, the

authors introduced a new SMP testing method for optimizing the response of SMPs (32). Keeping with the trend of SMP property tuning, Liu and coworkers (33) ingeniously adjusted the T_g of an otherwise high-T_g network by adding a plasticizing miscible polymer to yield a single-phase interpenetrating network (IPN). In particular, a hydrogen-bonding network from copolymerization of methyl methacrylate, N-vinyl pyrrilidone, and crosslinked with ethylene glycol dimethacrylate was blended with poly(ethylene oxide) (PEO) to yield an attractive T_g of 50°C. Near-perfect fixing and recovery (>99%) were achieved for the IPNs. The same materials will likely be moisture sensitive and may allow for water-triggered SM, as discussed in reference to the Jung et al. work (34). In a closely related effort, Yakacki and coworkers (35) prepared a family of covalent networks involving the copolymerization of methyl methacrylate with PEG dimethacrylate (PEGDMA) macro-cross-linkers of varying molecular weight. By varying both the incorporation level and the PEGDMA molecular weight, the researchers were able to independently vary the T_g of this miscible system [PEGDMA plasticizing poly(methyl methacrylate) (PMMA)] and the rubber elastic modulus for $T > T_g$. Using a range of quantitative SM characterization methods, Yakacki et al. (35) reported excellent shape recovery and fixing and found that the constrained recovery stress increased with increasing cross-linking density, as expected. The sharpness of the shape recovery event was quite variable but uniformly broad, among the compositions with reasonably low T_g. Because medical applications were targeted by such compositions, biocompatibility testing was conducted. Unfortunately, the results of this testing were not detailed in the publication (35).

SMPs have also found use in structural applications in which epoxy-based materials are often used owing to their intrinsically high mechanical properties, chemical resistance, thermal stability, and tunable transition temperatures. Elastic memory composites (EMCs) recently developed by Composites Technology Development, Inc. are an example of such materials (36). However, little information regarding their synthesis and curing kinetics is available. Merline et al. (37) investigated the cross-linking reaction and curing kinetics of an epoxy resin with an amine telechelic polytetramethylene oxide (PTMO). They claimed first-order kinetics. Variation in network composition led to transformation temperatures ranging from 77°C to 110°C. The authors reported that the better crystallization and/or dipolar interactions afforded by cross-linking with PTMO improved the SM properties. The shape recovery reached 99%, and the recovery times ranged from 12 to 30 s for simple bending deformations.

Chung and coworkers (39) reported surprising reversible actuation for semicrystalline and covalently cross-linked poly(cyclooctene) (38) when thermally cycled about the melting transition under a constant tensile load. The researchers observed that crystallization of this polymer under an applied tensile stress of ~1.0 MPa resulted in an incremental tensile strain above that of the isotropic elastic strain in the range of 20% to 40%. Upon heating at the same load, this incremental strain was reversed nearly completely (>98%) as the melting transition was surpassed. Dispersing the same materials with a fluorescent, chromogenic oligo(*p*-phenylene vinylene) dye, Kunzelman et al. (8) revealed reversible color changes during one-way SM cycling about the materials melting transition. Using large, nonpolar ($-C_{18}H_{37}$) endgroups for the dye design imparted it with significant solubility; however, the solubility was restricted to the amorphous phase whose volume fraction decreased during crystallization. Consequently, the same phenomena responsible for shape fixing—namely, crystallization—caused dye aggregation and excimer formation so that the fluorescing color of the polymer under UV illumination dramatically changed from green to orange. So, transient strain fixing and color change occurred simultaneously. Conversely, heating such samples above T_m led to strain recovery together with a fluorescent color change back to green, with seemingly high spatial resolution.

Shape Memory Polymers with New Fixing Mechanisms

Researchers have unveiled new macromolecular design concepts that engender unique shape fixing mechanisms. In one approach, Merline et al. (40) used improved intermolecular interactions through H bonding as the strategy to improve SM behavior of their PTMO/poly(acrylic acid–coacrylonitrile) [P(AA-co-AN)]-complexed gel. They measured an increase in E'_g/E'_r with increasing H bonds and observed that the SM properties varied linearly with the content of H bonds. The enhanced SM performance resulted from the enhanced coupling between the reversible phase (PTMO complex) and the fixed phase [cross-linked P(AA-co-AN)] achieved through H bonding.

H bonding by the self-complementary H-bonding group ureidopyrimidinone (UPy) (41) was proven capable of strain fixing in a covalently cross-linked butyl acrylate elastomer (42). Using lightly cross-linked networks with only 2% UPy groups, Li et al. proved that fixing levels of 90% were achievable—much greater than for the comparable photofixing approach discussed elsewhere (43)—and that strain recovery was nearly complete, although very broad. For such materials, the secondary reversible network (in this case established by H bonding) set for one shape competes with the primary covalent network with a distinct equilibrium shape. Above any separate vitrification or crystallization event, fixing should be determined by the relative cross-link densities of the primary and secondary networks, although this aspect was not investigated.

Lendlein and coworkers (43) elaborated an exciting concept of photo-triggered fixing and recovery in two distinct covalently cross-linked networks. Soft copolymer networks consisting of thermally polymerized *n*-butyl acrylate (BA) and hydroxyethyl methacrylate (HEMA) ($T_g < 20°C$) were cross-linked with a dimethacrylate compound and further copolymerized with a cinnamic acid (CA) terminal to a hydroxyethyl acrylate (HEA) monomer. Such networks enabled a new, reversible irradiation-based SM effect functional without external heating or cooling (**Figure 2**). Shining intense light ($\lambda > 260$ nm) on the stretched elastomers caused [2 + 2] cycloaddition reaction between adjacent CA groups that served as temporary cross-links in addition to the original cross-links. Thus, releasing the load following 1 h of light exposure yielded stable strain fixing in the range of 10% to 30%, increasing with CA amount. Subsequent exposure to higher energy light ($\lambda < 260$ nm) reversed the cycloaddition reaction and prompted good recovery of the original strain over the course of 1 h. Although this process is quite slow, the functionality of this concept is attractive through its enabling of remote and room temperature operation. This approach appears restricted to elastomers owing to the innate competition between primary covalent cross-links and labile photoaddition cross-links. Thus, the mechanical function of the fixed state will likely limit applications to those typical of elastomers.

In another approach toward reversible but covalent cross-linking, Ishida et al. (44) reported on reversible networks consisting of furan-terminated telechelic polyesters of poly(1,4-butylene-succinate-*co*-1,3-propylene succinate) reacted by Diels-Alder (DA) addition with a trifunctional maleimide (**Figure 3**). Depolymerization of the network structure occurred at an elevated temperature of 140°C, but repolymerization could occur above or below the polyester melting temperature, resulting in dramatically different elastomer stiffnesses. Although the potential for SM characteristics of these materials was not discussed, it is apparent that this chemistry represents a very attractive approach toward reconfigurable, T_m-triggered, SM elastomers.

Covalent networks combining network strands with distinct fixing temperatures and even distinct mechanisms (T_g and T_m) enable sequential fixing of two shapes and subsequent recovery (on heating) of the same shapes in reverse order (45). Three shapes are witnessed upon heating: twice fixed, once fixed, and equilibrium, and thus the materials are referred to as triple shape. One system (of two) reported combined T_g- and T_m-based SM of widely separated transition temperatures, whereas the other system combined two T_m-based SM mechanisms quite close in proximity.

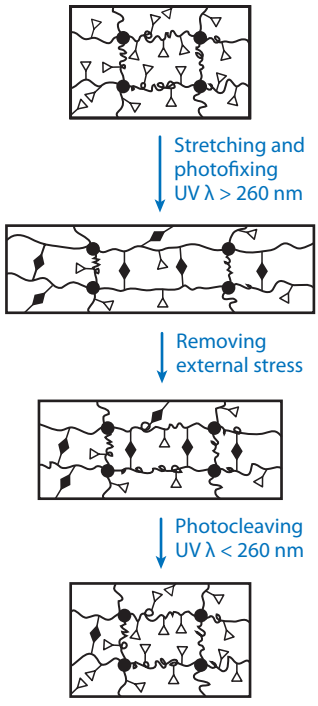

Figure 2

Photofixing and photocleaving scheme to achieve light-activated shape memory. Adapted with permission from Reference 43.

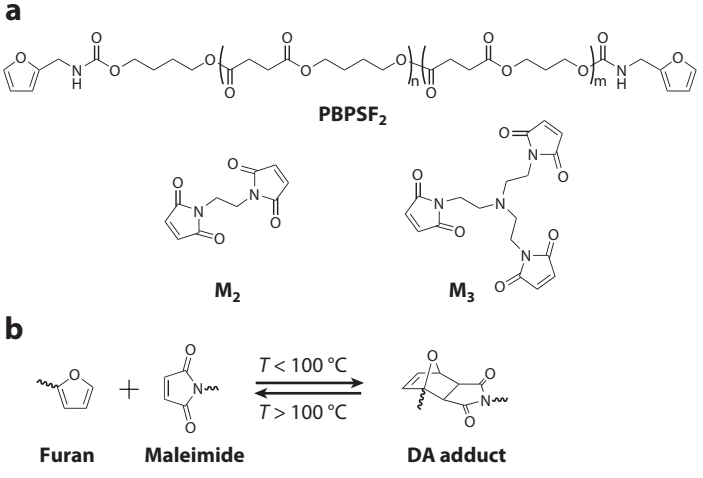

Figure 3

Reversible cross-linking scheme via Diels-Alder (DA) chemistry enabling thermal resetting of a covalent network structure. PBPSF2, furyl-telechelic poly(1,4-butylene succinate-*co*-1,3-propylene succinate. Reproduced with permission from Reference 44.

The former case was accomplished by conetwork formation of a PCL crystalline phase and a poly(cyclohexyl methacrylate) amorphous phase, whereas the latter was enabled by copolymerization of PEO comb chains (graft copolymer of mPEG-methacrylate) with PCL dimethacrylate. In both embodiments of such triple-shape materials, the first fixing event (on cooling) was generally worse than the second fixing event. Demonstrations revealed unique sequential SM functionality, including opening of a large-diameter tube from a flat shape, followed by shrinking of the tube diameter (fixed initially to be large) to a smaller equilibrium size. It appears that the only requirement for such materials is a conetwork system with two interpenetrating phases (that are mechanically percolating), so it is likely that numerous other examples will come forth in the future and that applications will abound.

Most recently, molecular interactions in ionomers have been exploited to produce novel SMPs. Weiss et al. (46) described the inclusion of fatty acid salts within a sulfonated ethylene propylene diene monomer (EPDM), a thermoplastic elastomer that was developed by Exxon in the mid-1970s. The materials exhibited SM, although not optimal, properties. Variation of the fatty acid salt (i.e., melting temperature) allowed for systematic variation of the transformation temperature of the SMP from 20°C to 120°C. The fatty acid salts, while acting as a plasticizer at higher temperatures, also acted as physical cross-links and fillers at lower temperatures when crystallization occurred. The authors postulated that the fixed phase of the SMP resulted from the nanophase separation of the elastomeric ionomer, whereas the reversible phase was due to the melting and crystallization of the fatty acids. By comparison, Han et al. (47) developed semicrystalline multiblock copolymers containing sulfonate groups in one block, revealing T_m-based SM behavior that benefits from ionic physical cross-linking. Testing revealed relatively slow fixing [owing to limiting crystallization kinetics of the poly(butylene adipate) block] and good shape recovery, with R_r increasing with each SM cycle from 80% to 90% and then to 95%.

Nanocomposite Shape Memory Polymers

Most areas of polymer research have seen the impact of nanoscale reinforcement, and SMPs are no exception. In one example, Auad and coworkers (48) took the unique approach of filling a polyester-based thermoplastic polyurethane with nanocellulose whiskers, seeking enhancement of material stiffness. Accordingly, nanocellulose whiskers were dispersed using a solvent method [dimethyl formamide (DMF)] at loadings up to 1 wt% in a semicrystalline polyurethane with T_m (for fixing and recovery) of 41°C. Poor strain fixing (<50%)—despite an enhancement of the degree of crystallinity—and modest strain recovery (~90%) were reported, with very little impact on these characteristics in response to nanocellulose addition. An impressive 50% increase in room temperature tensile modulus was observed at 1% loading—a reflection of the nanoscale reinforcement approach utilized. In another approach to nanocomposite SMPs, Gunes et al. (49) investigated the preparation and performance of PCL-based TPUs incorporating a variety of inorganic fillers, most notably the organically functionalized aluminosilicate clay Cloisite 30B. The base resin featured a hard-block content of 33 wt% and relatively poor SM performance in the unfilled state: $R_f = 93\%$ and $R_r = 80\%$ (for 100% strain). The dispersion of clay within the TPU maintained these SM performances, whereas other fillers disrupted the soft-segment crystallization and hampered strain fixing. Importantly, clay increased the recovery stress exhibited during constrained recovery through T_m from 2.4 to 3.12 MPa for 100% strain fixed. By comparison, Kim et al. (50) prepared and studied T_g-based, amorphous SMP nanocomposites through use of an intercalated polymerization initiator within sodium montmorillonite (MMT) clay galleries and polymerization of ethyl methacrylate. The resulting materials featured a T_g in the range of 55°C to 72°C (increasing with MMT content) and a modest rubber elasticity above T_g. The shape fixing

was in excess of 90%, whereas the shape recovery improved with cycling, more so with increased clay loading, although R_r values were not reported.

As a bottom-up nanocomposite approach, Lee et al. (51) reported covalent nanocomposite networks combining PCL and POSS to yield a T_m-based SMP. In particular, a crystallizable POSS diol was utilized as a ring-opening polymerization initiator of CL, and the nanostructured/hybrid POSS was architecturally placed precisely in the center of each chain and then end-capped with the acrylate groups. SM networks were then achieved by cross-linking with a tetrathiol cross-linker in the presence of a photoinitiator. For a series of compositions ranging from 22 to 49 wt% POSS, the materials exhibited phase behavior dominated by either PCL crystallization or POSS crystallization, depending on composition. A particular composition exhibiting crystalline POSS with a sharp melting transition (42 wt% POSS; $T_m = 86°C$) and amorphous PCL was examined for SM characteristics, revealing excellent fixing (>99%) and recovery (~99%) with an associated modulus plateau below T_m that is quite flat, thus enabling very sharp recovery.

Thermomechanical Conditioning of Shape Memory Polymers

Recent studies have found that the performance of an SMP can be dramatically impacted by the applied thermomechanical cycling conditions. In other words, the desired SM properties of a given composition can be obtained by thermomechanical conditioning. Hu et al. (52) comprehensively investigated the effect of various thermomechanical conditions on strain recovery. These researchers revealed the existence of optimum deformation temperature, leading to recoverable strains greater than 80%, which ranged from $T_g - 10°C$ to $T_g + 50°C$. Furthermore, recovery began most dramatically at the prior deformation temperature. In addition, time-dependent viscoelastic effects such as stress relaxation may also influence the recoverable strain. Hu et al. (52) observed, in particular, that shape recovery decreased as strains increased from 100% to 300% and as strain rate was decreased. Morshedian et al. (53) conducted a similar experimental study on a lightly cross-linked low-density polyethylene (LDPE) system and found good correlation between occurrences of stress relaxation and irrecoverable strain. This finding led these investigators to develop a viscoelastic model (discussed in Shape Memory Modeling, below). Tobushi et al. (54) systematically studied the irrecoverable strain of a SMPU as a function of strain holding time, t_h, and deformation temperature, proposing an empirical relationship describing irrecoverable strain relative to holding strain, S, as

$$S = S_P \left(1 - e^{-((t_h - t_s)/c)}\right), \quad 1.$$

where S_P, t_s, and c are the saturated value of S, the critical time before irrecoverable strain appears, and a time constant, respectively. S_P, t_s, and c are determined experimentally and vary with the irrecoverable strain, the holding strain, and the holding time at a given deformation temperature. In addition, Tobushi et al. (52) proposed to control the amount of irrecoverable strain so as to obtain a desired new shape different from both the permanent and the first temporary shape, a technique termed secondary shape forming.

Similarly to recoverable strain, the recovery stress may also be affected by thermomechanical conditions. Here, the recovery process, termed constrained recovery, involves heating under conditions of fixed strain while stress evolution is observed (64–66). Gall et al. (55) studied the SM behavior of an epoxy-based SMP and found that the recovery stress depends largely on the deformation temperature of the sample. The sample deformed at a higher temperature ($T_d = 1.25\ T_g$) showed a simple sigmoidal increase of stress upon heating, whereas the sample deformed at a lower temperature ($T_d = 0.75\ T_g$) exhibited a peak in recovery stress with a much higher magnitude than that expected for the final stress as dictated by the modulus at $T > T_g$. Similar

observations of a recovery stress peak during constrained recovery have been reported for SMPs under compression (65, 67), tension (56), three-point bending (55, 57), and shear (57). In contrast to Tobushi et al. (54), this phenomenon was explained in terms of thermal expansion (56) and structural relaxation during the glass transition (58).

The recovery temperature was also found to depend on thermomechanical conditions, especially the deformation temperature. As reported by Gall et al. (55), the recovery temperature of a highly cross-linked epoxy (T_g-based) SMP deformed at $T_d = 0.75\ T_g$ was substantially lower than that of the same material deformed at $T_d = 1.25\ T_g$. Yakacki et al. (31) applied this principle to a series of SMP stents. They achieved almost complete recovery at 37°C by deforming the stent at room temperature even though the T_g of the materials ranged from 52°C to 55°C. Khonakdar et al. (59) observed a similar phenomenon for a T_m-triggered SMP. In this case, they explained the phenomenon in terms of the thinner crystallites formed at a lower temperature, which in turn melt at a lower temperature.

Yakacki et al. (32) introduced the notion of a deformability peak in an attempt to maximize the SM response of polymers. Their new protocol for SMP testing is based on the understanding of the relationships between strain-to-failure, temperature, and polymer structure. The deformability peak corresponds to the peak in the strain-to-failure envelope of a material at varying temperature. In the deformability peak region, the material has optimal resistance to microcracking, owing to viscoelastic toughening, as well as the highest achievable strains. Therefore, an optimum deformation temperature should be selected within the temperature window of the deformability peak. For their acrylate-SMPs, the authors found the deformability peak was located at the glass transition onset.

Triggering Mechanisms

Although direct heat remains the main trigger of SM behavior in polymers, such an approach is not always practical. This opened the door to searching for alternative triggering mechanisms. Irradiation [UV, solar, infrared (IR)], electrical current, or magnetic field have been used. Another method involves a shifting of an SMP transformation temperature during usage via molecular interaction with a surrounding solvent. For example, Yang and coworkers (60) effectively activated shape recovery of their ether-based SMPU at room temperature by immersion in water. By disrupting the intramolecular H bonding and acting as a plasticizer, water depressed T_g by 35°C and hence effectively allowed for room temperature actuation. Concurrently, however, the width of the transition increased from approximately 10°C to 40°C, thus leading to a decrease in shape recovery as well as recovery stresses. A similar approach was adopted by Lv et al. (61), who used DMF to trigger the SM response of a commercial styrene-based SMP. Although these solvation techniques effectively reduce T_g, allowing for room temperature actuation, the use of solvents may be undesirable for most applications. Moreover, the repeatability over consecutive cycles becomes questionable because fixing of a temporary shape would require solvent removal from the SMP.

By modifying chitosan (85% deacetylized) with PEG plasticization and diepoxide cross-linking, Chen and coworkers (62) unveiled a unique composition capable of strain fixing through crystallization and rapid strain recovery by hydration. Focused on the vascular stenting application, the researchers processed spiral coils of chitosan/PEG strands that were then chemically fixed by cross-linking to set the equilibrium shape. A subsequent exposure to water led to rapid hydration and concomitant radial expansion in a short period of 150 s with a 1-N expansion force. Although it is unlikely that water swelling of the samples was able to be completed in this timeframe, the spiral geometry may have allowed expansion as a consequence of surface hydration alone, although the authors did not offer an explanation for the rapid kinetics. Also in the area of solvent-induced

strain recovery, Jung and coworkers (34) collaborated with one of us (P.T.M.) to demonstrate water-induced shape recovery in a PEO-based polyurethanes bearing the strongly hydrophobic POSS moiety in the hard segment (16). Hard-segment contents of 30 to 50 wt% and a PEG molecular weight of 10 kDa were utilized. Bending strains that were fixed by crystallizing the PEO soft phase were recovered incompletely (65–85%) over the course of 300 s at 30°C. Improvements in this recovery are expected for TPUs with smaller hard-segment content or larger PEG molecular weight.

Researchers have reported more promising triggering mechanisms that involve indirect heating through the application of an external stimulus. Small et al. (63–65) used IR activation to allow safe in vivo deployment of SMP stents or SMP foams. For this purpose, these investigators studied the SM behavior of a commercial SMPU doped with various laser-absorbing dyes [e.g., indocyanine green (ICG) or Epolight 4121]. Their study of the ICG-doped SMPU in air showed promising results with full recovery in ~5 s under irradiation at 800 nm and 900 to 1100 mW. They found that the optimum concentration of ICG in this case ranged from 0.08 to 1.56 μM (64, 65). Yu & Ikeda (66) recently reviewed the various classes of polymeric systems developed for photo-actuation. They discussed the UV activation of polymer gels as a result of a change in osmotic pressure and the visible and IR activation of polymer gels as a result of indirect temperature changes. The UV-Vis activation of photochromic amorphous systems such as monolayer, gels, and films was also reviewed. In this case, the isomerization of incorporated chromophores leads to molecular shape changes and/or dipole moment changes that translate into macroscopic shape changes. Yu & Ikeda (66) discussed research conducted on active liquid crystalline elastomers responding to irradiation through isomerization of embedded chromophores or to temperature gradients resulting from limited photon absorption. Finally, these researchers also reviewed the recent study by Lendlein et al. (43) that showed photoresponsiveness of polymer networks incorporating functionalities that covalently bond or debond upon irradiation at specific wavelengths in the UV or visible range.

The use of electric currents as a triggering means for SM effect has also proven successful and was recently reported by Sahoo et al. (12, 67). Their initial work involved the use of a conductive polymer [polypyrrole (PPy)] as a coating layer of their in-house thermoplastic SMPU. At the percolation threshold of the PPy layer (10% loading), the electrical conductivity increased from 0.053 to 0.09 S cm^{-1}. At 20% loading under a 40-V electric potential, 85% to 90% recovery was achieved in ~25 s. A lower loading led to higher shape recovery with a slight rate penalty. This was explained by the combination of increased soft-segment crystallinity, tensile strength, and elongation at break at lower PPy content and the loss of integrity of the PPy network during deformation. Later, the authors investigated the effect of incorporating a combination of MWNTs and/or PPy (12). The highest electroconductivity (0.098 S cm^{-1}) and highest shape recovery (90% to 96%) were achieved for the samples containing 2.5 wt% of PPy (coating layer) and 2.5 wt% of dispersed MWNTs within the SMP matrix. Recovery was achieved within 20 s after application of the electric field. Interestingly, although not discussed by the authors, the relatively high rubbery modulus of this material (110 MPa) may support higher recovery stress applications. Ratna & Karger-Kocsis (6) reviewed other conductive fillers, such as vapor-grown carbon fibers and carbon black, among others, used for electroactuation of SMPs.

Using styrene-based thermoset SMPs, Leng et al. pursued the possibility of an electrically conductive SMPs suitable for resistive heating for the triggering of recovery (68). A combination of carbon black nanoparticles and short carbon fibers was used, leading to an impressive electrical conductivity of $\sigma = 2.3$ S cm^{-1} with 5% carbon black and 2% short carbon fibers. Unfortunately, no electrically stimulated shape recovery was reported. It is hoped that research like this will persist to the desirable outcome of an electrically triggered SMP. Significant progress was made in the preparation of partially conductive SMP blends through the dispersion of micrometer-scale nickel particles in a commercial SMP, Diaplex MS-5510 (69). Ni particles (5–7 μm) were dispersed in

the SMP using a solvent process in conjunction with magnetic-field alignment that led to particle chaining and adequate resistive heating capacity. Joule heating of samples containing 10 vol% Ni raised the specimen temperature above T_g, inducing strain recovery (in flexure) in 90 s for samples of a particular dimension. At this significant loading, there is likely a compromise on strain limit of elastic response above T_g, though this aspect was not investigated. Additionally, there is certainly a benefit to the thermal conductivity of the SMP composite, even for thermal triggering.

Finally, electromagnetic actuation appears to have attracted the most interest recently. In this phenomenon, heat is generated through power losses of a magnetic filler. Reports have mostly focused on the actuation of SMPs targeting medical applications; however, in many cases, the field strengths and frequencies largely exceed those applicable in medical applications. Indeed, recent reports show magnetically driven actuation using high frequencies and power ranging from 258 to 1400 kHz and 5 to 14 W, respectively (58–60). The strategies involved in material development are the incorporation of magnetically responsive fillers such as terfenol-D particles (70), Fe_2O_3/silica particles (71), Ni-Zn ferrite particles (6), and Fe_3O_4 (i.e., magnetite) particles (72) within an SMP matrix. For instance, although incomplete, fast recovery for both the magnetite-filled acrylate-SMP ($t_r = 20$ s) developed by Schmidt (72) and the terfenol-D-filled commercial SMPU ($t_r = 90$ s) prepared by Hazelton et al. (70) was achieved. Better shape recovery (~91%) was achieved by Mohr et al. (71), who effectively triggered SM under varying field strengths of their Fe_2O_3/silica particle-filled SMPU with a shape fixity ranging from 98% to 118%.

Thermal triggering of a SM polyurethane (Diaplex MP5510) (erroneously stated to be T_m based) was achieved by inductive heating of samples filled with nickel zinc ferrite at levels of 10 and 20 wt% (73). Interestingly, the particles selected were designed to feature inductive heating through the mechanism of magnetic hysteresis (instead of Eddy current) so that control of temperature at the Curie temperature, T_C, could be assured. Although autonomous temperature control like this is an attractive concept, the temperatures achieved during exposure to 10 MHz electromagnetic fields were far below T_C, and modest temperature rises of 11°C and 7°C in 45 s at 20 wt% and 10 wt%, respectively, were observed. In principle, this method of noncontact thermal triggering is very attractive for surgical deployment of SMPs; however, significant improvements are needed in efficiency of inductive heating and at frequencies safe for human tissue, or 50–100 kHz, as noted by the authors.

Razzaq et al. (74) more recently reported on a more viable electromagnetic actuation mechanism of a microsized magnetite-filled SMPU, using a lower frequency and field strength (50 Hz and 4.4 kA m^{-1}). Actuation was possible at lower field frequencies owing to the heat generation mechanisms involved with microsized magnetite. The SM response, however, was much slower than in other reports, with initiation of recovery at 4 min and full recovery at 20 min. Progress is still needed in the area of triggering mechanisms to develop viable solutions for a wide range of applications with targeted SM properties such as response speed, shape fixing, and shape recovery.

SHAPE MEMORY MODELING

The majority of the research efforts on SMPs carried out in the past have concentrated on experimental work, including developing new chemical compositions, characterizing SM performance, and designing SMP-based devices for novel applications. Relatively few studies have committed to mathematically modeling the SM behavior. Among those studies using mathematical modeling, two approaches have generally been used. The first approach utilizes standard linear viscoelasticity. It models the SMP with a combination of elastic and viscous units with temperature-dependent parameters. Using this approach, Morshedian et al. (53) developed a three-element model consisting of a Voigt unit (E and η_1) and a single dashpot (η_2 with $\eta_2 \gg \eta_1$) connected in series to

predict the relationship between stress relaxation and irrecoverable strain for a lightly cross-linked LDPE system. During stress relaxation at T_b ($T_b > T_{trans}$), the Voigt unit, initially bearing the total deformation strain, gradually transfers the strain to the single dashpot η_2 while the total strain is held constant, following the derived equation:

$$\eta_1 \frac{d\gamma}{dt} + E\gamma = \sigma_0 \frac{1 + \frac{\eta_1}{\eta_2}}{1 + \frac{\eta_1}{\eta_2} + \frac{t}{\tau}}, \quad 2.$$

where γ, t, and σ_0 are the strain of the Voigt unit, the strain holding time, and the initial stress before relaxation, respectively. τ is the system relaxation time with $\tau = \eta_2/E$. Because the strain transferred to η_2 is dissipated in the viscous process, it becomes irrecoverable. Using the same model, Khonakdar et al. (59) simulated the complete shape recovery process by introducing temperature dependency to η_1. Buckley et al. (75) adopted a generalized Voigt model with temperature-dependent retardation times and relaxed compliance. The model was able to predict T_{max}, the temperature at which the maximum recovery rate is achieved, and ΔT, the temperature window, and thus the sharpness of the recovery transition, on the basis of normalized retardation spectra obtained from experimental creep curves. Variation in cross-link density and cross-linker led to variation in retardation times and hence in T_{max} and ΔT, as the model predicted.

The second general approach is based on the perspective of thermodynamics associated with SM behavior. Here, the SM behavior is believed to be due primarily to a transition from an entropic rubbery state (above the transition temperature, either T_m or T_g) to an internal energy–dominated state (below the transition temperature, either glassy or semicrystalline). In the rubbery state, the deformation mainly causes a change in entropy, and the resulting stress can be determined by the entropic rubber theory. In the glassy (or semicrystalline) state, the entropic change is "locked" owing to a decreased mobility of individual polymer chains by a decrease in free volume or the presence of crystalline domains. Any resulting stress (at small strain levels; i.e., not considering yielding) is due primarily to changes in internal energy. Therefore, the entropic stress generated in the rubbery state is frozen, or stored, and can only be released by heating above T_{trans} to reactivate the entropic changes. Under this general concept, various researchers have undertaken a mixture or biphasic approach, in which an SMP is represented as a mixture of two phases: a hard, internal energy–dominated frozen phase and a soft, active phase dominated by entropy changes. A rule of mixtures is applied, and the transition of state is modeled as a change of relative volume fractions of the two phases, with the use of a state variable (usually the fraction of one phase). The constructed model is then loaded with a prescribed thermomechanical setting and material properties input and used to represent the SM response by solving of the derived constitutive equations.

Liu et al. (56) based their work on a biphasic mixture model similar to that described above. The strain of both phases is decomposed into three parts:

$$\boldsymbol{\varepsilon} = \boldsymbol{\varepsilon}_\mathbf{S} + \boldsymbol{\varepsilon}_\mathbf{m} + \boldsymbol{\varepsilon}_\mathbf{T}, \quad 3.$$

where $\boldsymbol{\varepsilon}_\mathbf{S}$, $\boldsymbol{\varepsilon}_\mathbf{m}$, and $\boldsymbol{\varepsilon}_\mathbf{T}$ are the elastic strain stored in the frozen phase, the mechanical strain, and the thermal strain, respectively. Both the frozen and the active phases were modeled as linear elastic solids following the generalized Hooke's laws, that is:

$$\boldsymbol{\sigma} = (\phi_f \mathbf{S_i} + (1 - \phi_f)\mathbf{S}_e)^{-1} : (\boldsymbol{\varepsilon} - \boldsymbol{\varepsilon}_\mathbf{S} - \boldsymbol{\varepsilon}_\mathbf{T}), \quad 4.$$

where φ_f, $\mathbf{S_i}$, and $\mathbf{S_e}$ are the frozen-phase fraction, the elastic compliance tensor for the frozen phase (internal energy), and the elastic compliance tensor for the active phase (entropic change), respectively. During the phase transformation (glass transition), it is assumed that the newly formed frozen phase inherits the elastic strain of the active phase at that moment ($\boldsymbol{\varepsilon}_\mathbf{m}$ of the active phase

transfers to ε_s), and the temperature derivative of ε_S can be obtained by

$$\frac{d\varepsilon_S}{dT} = \mathbf{S_e}(T) : (\phi_f \mathbf{S_i} + (1-\phi_f)\mathbf{S}_e)^{-1} : (\varepsilon - \varepsilon_S - \varepsilon_T)\frac{d\phi_f}{dT}. \quad 5.$$

Finally, the glass transition process, characterized by φ_f(T), is given by a phenomenological function:

$$\phi_f = 1 - \frac{1}{1 + c_f(T_h - T)^n}. \quad 6.$$

The two variables c_f and n are determined experimentally via data fitting. By use of two internal state variables, the frozen-phase fraction (φ_f) and stored entropic strain (ε_S), the glass transition and the simultaneous strain storage/release process can be mathematically represented. The authors found that the one-dimensional equations derived from Equations 3 to 6 for uniaxial deformations reasonably represented the small strain SM response of an epoxy-based SMP in compression, in tension, or under no strain. They also demonstrated the applicability of the model for predicting the SM response under different flexible external constraints.

Qi et al. (58) developed a constitutive model based on a similar biphasic mixture assumption. The rubbery phase and the glassy phase were modeled with (*a*) a hyperelastic spring (Arruda-Boyce eight-chain model) and (*b*) a parallel combination of a hyperelastic spring and a viscoplastic component, respectively. The glass transition was treated similarly as did Liu et al. (56) by introducing temperature dependences of the rubbery and glassy phase fractions using a phenomenological function. The temporary shape is fixed by the newly formed glassy phase, which takes the current configuration of the rubbery phase as its initial configuration. The model also considered the redistribution of the deformation in the material due to the evolving phase composition. The model can predict well the different stress-strain behaviors at different temperatures (above and below T_g) as well as the unconstrained recovery response of a T_g-activated SMP under compression. However, discrepancy between the model and the experimental results was observed for constrained fixing and recovery. Experimental results revealed stress decay well below T_g during shape fixing and a distinct peak during constrained recovery. The model failed to capture either feature. This was rationalized by the authors (58) by delayed heat transfer and structural relaxation events during the glass transition. Another model, arguably more physically meaningful, was developed by the same group of authors by incorporating the time-dependent effects of both structural relaxation—using a nonlinear Adam-Gibbs model—and stress relaxation (76). A better prediction of stress evolution during constrained recovery process of a compressed SMP plug was achieved, as shown in **Figure 4** for the case of a cross-linked poly(*t*-butyl acrylate) SMP. The authors also analytically evaluated the individual effects of structural relaxation and stress relaxation on shape recovery and found that they mainly affect the onset of strain recovery and recovery time (sharpness), respectively.

In another work conducted by Diani et al. (77), a more thermodynamically driven framework was constructed. The transition from an entropic rubbery state to an internal energy–dominated glassy state was modeled by considering a heterogeneous material, represented as a Zener model, having two different deformation mechanisms, represented by an elastic component (for entropy) and a viscoelastic component (for internal energy). The deformation gradient, therefore, split into an elastic part and a viscous part, the evolution of which was determined on the basis of thermodynamic requirements (satisfying Clausius-Duhem inequality). The model favorably predicted the experimentally measured stress evolution during constrained shape fixing and recovery steps (56). Chen & Lagoudas (78) developed another constitutive theory in the framework of classical nonlinear thermoelasticity for large deformations. The history dependency of the material was incorporated into the model by using the frozen reference configuration concept with the use of

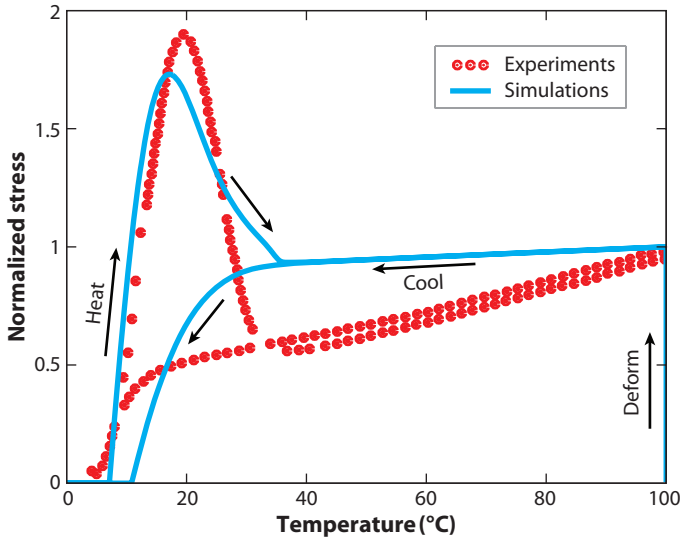

Figure 4

Comparison of simulation and experiment for the stress resulting from constrained recovery of a cross-linked, glassy shape memory polymer. The sample was compressed at 100°C and then cooled and reheated at constant platen separation, leading to a complex stress response that was well modeled. Adapted with permission from Reference 76.

an internal state variable describing the volume fraction of the frozen phase. Chen & Lagoudas (78) also derived a linear constitutive model from the nonlinear theory by assuming small deformations and examined the model by comparing it with the experimental data from Liu et al. (65, 72).

The models discussed above were all applied to T_g-activated SMPs. Relatively fewer studies have focused on T_m-activated SMPs, even though similar thermodynamic approximations could hold. Barot & Rao (79) employed a widely used framework known as multiple natural configurations to model SM response in T_m-activated SMPs. Within this framework, the amorphous and crystalline components of the SMP have their own natural configurations, or stress-free states. For the amorphous phase, regarded as an entropic rubber, the stress-free state would be the undeformed state corresponding to maximum entropy. For the crystalline phase, the assumption is that all crystals are formed in a stress-free state. In other words, the natural state, or the state corresponding to the lowest free energy of a crystal, is the state when the crystal is formed under strain during cooling. The tendency of each phase to return to its natural configuration represents the basis of the SM behavior in this approach. The model, with prescribed crystallization and melting kinetics equations, was applied to qualitatively represent typical SM cycles under both uniaxial deformation and circular shear. The model was able to capture most of the features exhibited by T_m-based SMPs. This model predicted an increase of strain during cooling under constant tensile stress (cooling-induced elongation), a somewhat counterintuitive phenomenon. However, this was observed experimentally by others and was utilized for two-way SM (39). In a later paper (80), Barot et al. extended the model to fit a full thermodynamic framework and derived constitutive equations that are invariant of mechanical stress and strain states, e.g., multiaxial and uniaxial, among others.

Kafka (81) took a different, "meso-mechanical" approach. His model considered an SMP as composed of two different continuous substructural components: a resistant component that

maintains elasticity with a constant Young's modulus and a compliant component that deforms in a time/temperature-dependent elastic-plastic-viscous manner. The internal variables, which describe the mechanical properties as well as the volume fractions of the two substructures, were estimated on the basis of experimental data and an approximation scheme. The model was demonstrated in a small strain SM system, but the concept appeared promising for future applications to large strain systems.

Because SMPs represent a class of polymeric materials having a large variety of chemical compositions, triggering mechanisms, and thermomechanical responses, developing a mathematical model, especially a generalized model for SMPs, is intrinsically difficult. Nevertheless, some progress has been achieved, as we hope we have shown. The interplay among thermodynamics, viscoelasticity, heat transfer, chain dynamics, phase transition, and other factors often results in complexity difficult to capture in tractable models, rendering a thorough analysis difficult. Given that most models are phenomenological in nature and only focus on certain aspects (e.g., thermodynamics versus viscoelasticity) while ignoring others for simplicity, the broad applicability of the models to predict experimental results under different conditions remains questionable. In fact a majority of the models discussed above were only applicable or tested for specific materials and/or a specific set of thermomechanical conditions (e.g., small strain). However, the ever-growing interest that SMPs have witnessed in the past several years and the ongoing research efforts that focus more on a fundamental phenomenological understanding of SMPs are signs that better, more in-depth understanding and modeling of SMPs is on the horizon.

APPLICATIONS AND FORMS

Researchers have proposed a myriad of potential applications for SMPs that include smart clothing, space and medical applications, smart structural repair, reconfigurable tooling (3), microelectromechanical systems, actuators, self-healing, health monitoring, biomedical devices (82), self-repairing auto bodies, kitchen utensils, switches, sensors, intelligent packing, heat-shrinkable tubes, and biosensors (6). Specific examples from recent works are detailed below.

Medical Applications

In a recent review, Dietsch & Tong (3) reported that 50% to 70% of the patents covering SMP technology target medical applications. Some of the current commercial sources that provide minimally invasive surgery solutions such as New Ortho Polymers, MnemoScience, and MedShape Solutions were cited. Also cited was All Fit China, which provides custom-fitted perforated medical casts. Although some commercial SMP solutions for applications in the medical field already exist, researchers are investigating new ways of using SMPs.

Ortega et al. (83) developed and studied an ingenious dialysis needle adapter wherein a compacted (fixed) SMP tube is threaded through the dialysis needle and expanded thermally (through blood contact) to yield an equilibrium shape that diverges in cross section. Following dialysis, the SMP adapter can be retracted through the needle. This flow geometry was designed to reduce intimal hypertension and stenotic lesions by reducing vascular wall shear stress through reduction of flow separation and associated flow oscillations. Model experiments and complementary simulation results clearly demonstrated the beneficial impact of using the SMP adapter on the streamlines from the needle shows the schematic design.

Many of the magnetically triggered SMPs discussed above targeted medical applications; they avoid the use of direct heat. Schmidt (72) discussed an interesting application in tumor therapy.

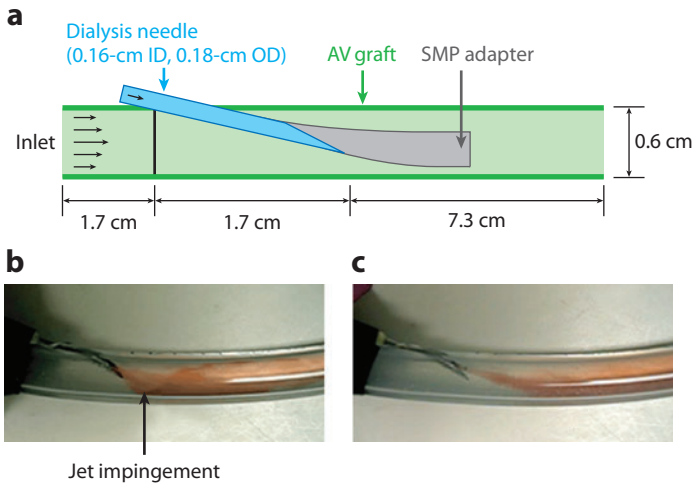

Figure 5

A shape memory polyurethane–based dialysis needle adapter. Shown is (*a*) the shape memory polymer (SMP) adapter design with the tubular adapter deployed and experimental flow visualizations (*b*) without and (*c*) with use of the SMP adapter, revealing desirable flow control. Adapted from Reference 83. ID, inner diameter; OD, outer diameter; AV, arteriovenous.

The magnetite-filled SMP could be inserted via minimally invasive surgery where needed. After deployment near the tumor, localized treatment is afforded, thus preventing unwanted heating of the surrounding healthy tissues as opposed to current techniques. Sharp et al. (84) described the use of a commercial epoxy as a self-deploying neuronal electrode. Their aim was to find a solution to minimize tissue damage during brain implantation (e.g., astrocytosis) that rapidly renders the probe deficient after implantation as well as to increase the compliance of the electrodes. Extremely slow rates of implantation have been promising in reducing postimplantation tissue damage. Although such rates are surgically impractical, SMPs would offer appropriate in vivo, postsurgical deployment rates. Although the shape recovery was low (35% after ~20 h), Sharp et al. (84) believe that adequate design may account for such small value. The measured recovery forces indicated that sufficient force up to 300 μm insertion depth could be achieved. Although such a device has not optimized, it certainly proved feasibility for this concept.

Several published reports have proposed the use of SM technology for thrombus removal. The main benefit lies in the fact that such SMP devices would replace the use of clot-dissolving drugs. Specifically, Small et al. (64, 65) described preliminary in vitro studies of a indocyanine green–doped SMPU that can be activated by IR irradiation. Fast recovery response in air ($t_r \sim 5$ s) was demonstrated. Preliminary calculations appeared to indicate that deployment in blood would require approximately 11 times more laser power. Also, Small et al. (85) developed an interesting prototype that uses the SM effect of both SMAs and SMPs. Here, the SMP served as a means of maintaining the straightening stress for endovascular delivery of the device as well as relaxing the stress to allow for actuation of the underlying NiTi. An electrical current provided for Joule heating of the SMA and, consequently, heating of the surrounding SMP. The SMP, adopting its low-modulus state, allowed for the NiTi phase transformation and hence for recovery from the straight shape to the corkscrew shape with $t_r = 5$ s in water at 0.8 A current.

Another medical application of SMP involves the treatment of endovascular embolization of fusiform aneurysms. Small et al. (63) developed a prototype that uses a combination of an SMP

stent and an SMP foam. There, the purpose of the stent was to maintain the lumen open in the parent artery while the foam activated the embolization of the aneurysm. This technique would provide a treatment solution of non-necked fusiform aneurysms as well as an alternative to the stent- and balloon-assisted coil embolization of wide-necked aneurysms. The triggering strategy involved photothermal actuation via laser irradiation of the IR-dye-doped commercial SMPU as allowed by the presence of the diffuser.

Light can be used to trigger the shape recovery of a vascular SMP stent through a photothermal effect wherein the light absorbed by a dye in a host polymer leads to heat production. Baer and coworkers (86) developed and studied a prototype vascular stent and deployment testing system that utilized a T_g-based thermoplastic SMPU, Diaplex MM5520, doped with a light-absorbing Pt-based dye. The equilibrium (stress-free) state was chosen to be that of an expanded diameter, and this stent was crimped with SM fixing on a fiber optic and combined light diffusion/SMP foam. Studies of light-activated deployment of the crimped state toward the expanded diameter were conducted in a unique artery model (silicone rubber tube) with and without blood simulant (water). The expansion was quite effective—possibly avoiding the need for balloon-aided expansion—but only at high power and without any water flow (convective cooling). The effect of the added dye on the biocompatibility of the system was not examined. We expect similar work to be pursued in the future with biodegradable and biocompatible polymers, ideally with built-in photothermal absorption capacity.

Sokolowski et al. (87) discuss a similar approach in their review of medical applications of SMPs. They showed encouraging in vivo testing of CHEM (cold hibernated elastic memory) foams for treating aneurysms. In addition, other benefits of SMP technology for biomedical applications were reviewed. First, SMPs offer a wide range of easily manufactured forms such as tubular mesh, foams, tubes, and coils. Second, SMP medical devices intrinsically would offer improvements to current technologies such as avoidance of arterial wall injury, custom fitting, and cost reduction. Similarity in mechanical properties (tan δ) of SMPs and of human skin would provide for a natural feel if SMPs were used as smart degradable bandages/wound closures, artificial skin, or implants. When used as stent materials, they could be designed to release embedded drugs, resulting in a decrease in restonesis and thrombosis after implantation. Sokolowski et al. (87) also discussed the possible use of SMPs as deployable elements of implants such as vascular grafts, cardiac pacemakers, and artificial hearts. Finally, these authors foresaw that CHEM foams or composites would be good candidates for the replacement of diseased arteries or scaffolds for tissue engineering especially for bone. Zheng et al. (88) also reported similar applications (i.e., orthopedics, bone implants, dental reparation).

SMP stents have been largely investigated in the past because they would allow for minimally invasive surgery and controlled deployment at body temperature. Yakacki and coworkers (31, 32) reviewed their advantages, such as the possibility of embedding drugs within stents to reduce rejection responses. Interestingly, they discussed the promises of SMPs for pediatric stenting in which the stent would grow with the patient, offering an evident competitive advantage over metal stents.

Space Applications

Sokolowski & Tan (36) provided an overview of conventional and SMP-based deployable structures for space applications. The authors reviewed the CHEM technology by describing their structure, advantages, and possible improvements. They described the benefit of using uniformly and evenly distributed micrometer-sized cells so as to enhance the mechanical properties and isotropy of properties of the resulting SMP. Moreover, they considered using solar blankets with

high ratio of solar absorptivity to IR emissivity as a new SM means. Some of the main applications discussed include nano-rover wheels for Mars applications, spring-lock truss elements for large boom structures, and solar sails that involve the use of CNT-loaded CHEM microfoams. The main advantage of using SMPs for space applications is that they would represent a large reduction in volume, weight, and cost compared with traditional self-deploying techniques. Interestingly, such SM systems could potentially be made of any form so as to produce systems and/or subsystems such as packages, tanks, rods, tubes, boom, wheels, and chassis (3). Another application involves the use of SMPs for aircraft morphing skins (3). Here, the SMP would provide for a continuous skin material that effectively transferred flight loads to the underlying structural members. Furthermore, upon activation the SMP would allow the internal structures to change shape and/or configuration. After activation the SMP would return to its high-modulus state, resume normal operation, and again bear structural load.

Textiles

Recently, interest has grown for smart textiles, as evidenced by increased reporting on the processing and characterization of SM fibers. Meng & Hu (11, 89) reported on the processing of PCL-based polyurethane melt-spun fibers. They showed that reinforcing the polymer with MWNTs proved useful for increasing the mechanical properties and hence the recovery stresses of the fibers, as well as for increasing shape recovery. Also discussed was the effect of hot versus cold drawing as deformation means in an attempt to mimic the deformation that occurs in textiles at room temperature upon creasing. Vili (90) reviewed the use of SMAs and SMPs for interior smart textile applications, especially for use as room partition, wall hanging, and window treatments. Although the author largely focused on manufacturing considerations, she indicated possible triggering mechanisms, such as temperature changes, sunlight, or electric currents. Moreover, she briefly reviewed commercial technologies that use SMPs for smart clothing. For example, she discusses the auto-sleeve-shortening shirt that was developed by Corpo Nove and the line of sports clothing by DiAPLEX (a subsidiary of Mitsubishi Heavy Industries), also mentioned by Dietsch & Tong (3). In the latter case, the activation resulted in opening of the fabric microstructure upon an increase in the surrounding temperature.

SMP fiber electrospinning, as an alternative to melt spinning, has also been investigated. Zhuo et al. (91) described the synthesis of electrospun SMPU fibers that reached 80% shape fixity and ~98% shape recovery at equilibrium. Interestingly, these fibers also exhibited changes in optical properties, hydroabsorbency, and water vapor permeability. As foreseen by the authors, this could open the door for applications as smart filters or membranes (i.e., novel temperature-sensitive membranes for water vapor permeability) if such fibers are assembled as nonwoven mats.

Structural Applications

As mentioned above, Dietsch & Tong (3) in a recent review discussed commercial sources of smart structural repair solutions based on SMP technology. These are manufactured under the trade names Rec'Repair™ and Rubb'n Repair™ by Cornerstone Research Group. Advantageously, these offer good conformability during application above their transformation temperature and higher resistance to peeling as well as higher structure integrity (compared with tape) after cooling to the service temperature ($<T_{trans}$). Other structural applications have been reported; for example, Schmidt (72) indicated the possibility of using their magnetite-filled SMP as a hot melt glue using microwaves as the triggering mechanism. Furthermore, Xie & Xiao (92) developed a self-peeling reversible adhesive that was based on epoxy-SMP and that, when combined with a

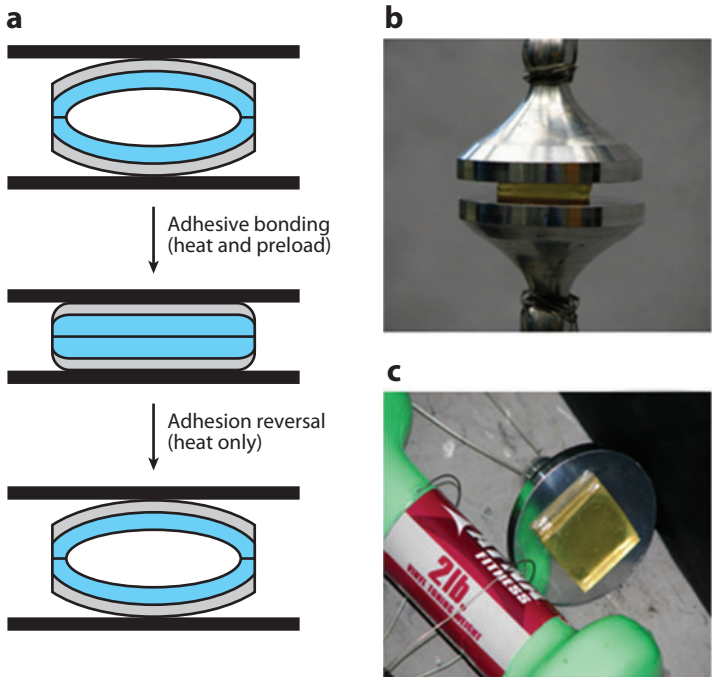

Figure 6

(*a*) Reversible adhesion through combination of a pressure-sensitive adhesive (*gray*) and shape memory polymer (SMP) (*blue*). (*b*) In the SMP fixed state, good adhesion is possible (60 kPa). (*c*) Because the SMP equilibrium shape is designed to be curved, thermally induced recovery allows facile peeling. Adapted from Reference 92.

pressure-sensitive adhesive, showed features similar to those of a gecko foot. Assembling the configuration shown in **Figure 6**, with a curved equilibrium SMP shape, and applying pressure above T_g yielded high pull-off strength (60 kPa). Heating above T_g triggered SMP recovery and self-peeling. The entire process can be repeated and thus offers a new paradigm in dry adhesives.

FUTURE DIRECTIONS

On the basis of our study of the recent research activity regarding SMPs, we can say with certainty that research in this area is flourishing with a high level of innovation (from molecular to device levels) and continued improvement in our understanding of underlying mechanisms at work. However, the field is far from mature, and we have observed a need for further research in a number of areas. In the area of SMP compositions, we see the need for new SMPs that allow precision tailoring of triggering breadth and recovery rate. Biodegradable SMP nanocomposites will require the incorporation of nanoscale fillers that are biocompatible or even resorbable. More attention is needed in the area of thermal and mass diffusivity enhancements and understanding for thermal- and solvent-triggered SMPs, respectively. The small thermal diffusivity of polymers remains a limitation, and improving thermal diffusivity without compromising elasticity presents a substantial challenge. Continued research in mechanics modeling is needed, particularly research focusing on accurate modeling of time-dependent and finite-strain SM phenomena. The current research trends point toward continued application development and innovations in the medical

arena. We anticipate with excitement similar efforts in the fields of architecture, sensors, and robotics.

SUMMARY POINTS

1. Research in the area of shape memory polymers (SMPs) is quite active and continuing to grow at a rapid rate.
2. Many new SMP compositions have been introduced and studied to reveal structure-property relationships and new shape memory mechanisms.
3. Significant attention is being placed on creative fixing and recovery mechanisms, including photo-activated and noncovalent or reversible covalent network formation.
4. Development and study of SMP nanocomposites have revealed significant advantages to be gained by polymer reinforcement at the nanoscale.
5. Application developments for SMPs are diverse, from vascular stents and neuronal probes to reversible adhesives and smart textiles.
6. The future for SMPs is bright, and we anticipate further expansion in the breadth of materials and the depth of our fundamental understanding and a diverse utilization of SMPs in a range of application areas.

DISCLOSURE STATEMENT

The authors are not aware of any biases that might be perceived as affecting the objectivity of this review.

ACKNOWLEDGMENTS

P.T.M. acknowledges support of the National Science Foundation under DMR-0758631.

LITERATURE CITED

1. Lendlein A, Kelch S. 2002. Shape-memory polymers. *Angew. Chem. Int. Ed.* 41:2034–57
2. Liu C, Qin H, Mather PT. 2007. Review of progress in shape-memory polymers. *J. Mater. Chem.* 17:1543–58
3. Dietsch B, Tong T. 2007. A review: features and benefits of shape memory polymers (SMPs). *J. Adv. Mater.* 39:3–12
4. Gunes IS, Jana SC. 2008. Shape memory polymers and their nanocomposites: a review of science and technology of new multifunctional materials. *J. Nanosci. Nanotechnol.* 8:1616–37
5. Mano JF. 2008. Stimuli-responsive polymeric systems for biomedical applications. *Adv. Eng. Mater.* 10:515–27
6. Ratna D, Karger-Kocsis J. 2008. Recent advances in shape memory polymers and composites: a review. *J. Mater. Sci.* 43:254–69
7. Rousseau IA. 2008. Challenges of shape memory polymers: a review of the progress toward overcoming SMP's limitations. *Polym. Eng. Sci.* 48(11):2075–89
8. Kunzelman J, Chung T, Mather PT, Weder C. 2008. Shape memory polymers with built-in threshold temperature sensors. *J. Mater. Chem.* 18:1082–86
9. Kelch S, Choi NY, Wang ZG, Lendlein A. 2008. Amorphous, elastic AB copolymer networks from acrylates and poly[(L-lactide)-*ran*-glycolide]dimethacrylates. *Adv. Eng. Mater.* 10:494–502

10. Razzaq MY, Frormann L. 2007. Thermomechanical studies of aluminum nitride filled shape memory polymer composites. *Polym. Compos.* 28:287–93
11. Meng QH, Hu JF. 2008. Self-organizing alignment of carbon nanotube in shape memory segmented fiber prepared by in situ polymerization and melt spinning. *Composites A* 39:314–21
12. Sahoo NG, Jung YC, Cho JW. 2007. Electroactive shape memory effect of polyurethane composites filled with carbon nanotubes and conducting polymer. *Mater. Manuf. Process.* 22:419–23
13. Xu JW, Shi WF, Pang WM. 2006. Synthesis and shape memory effects of Si-O-Si cross-linked hybrid polyurethanes. *Polymer* 47:457–65
14. Gunes IS, Cao F, Jana SC. 2008. Effect of thermal expansion on shape memory behavior of polyurethane and its nanocomposites. *J. Polym. Sci. B* 46:1437–49
15. Pierce BF, Brown AH, Sheares VV. 2008. Thermoplastic poly(ester urethane)s with novel soft segments. *Macromolecules* 41:3866–73
16. Knight PT, Lee KM, Qin H, Mather PT. 2008. Biodegradable thermoplastic polyurethanes incorporating polyhedral oligosilsesquioxane. *Biomacromolecules* 9:2458–67
17. Chen SJ, Cao Q, Jing B, Cai YL, Liu PS, Hu JL. 2006. Effect of microphase-separation promoters on the shape-memory behavior of polyurethane. *J. Appl. Polym. Sci.* 102:5224–31
18. Meng QH, Hu JL. 2008. Influence of heat treatment on the properties of shape memory fibers. I. Crystallinity, hydrogen bonding, and shape memory effect. *J. Appl. Polym. Sci.* 109:2616–23
19. Ji FL, Zhu Y, Hu JL, Liu Y, Yeung LY, Ye GD. 2006. Smart polymer fibers with shape memory effect. *Smart Mater. Struct.* 15:1547–54
20. Zini E, Scandola M. 2007. Shape memory behavior of novel (L-lactide-glycolide-trimethylene carbonate) terpolymers. *Biomacromolecules* 8:3661–67
21. Zhou SB, Zheng XT, Yu XJ, Wang JX, Weng J, et al. 2007. Hydrogen bonding interaction of poly(D,L-lactide)/hydroxyapatite nanocomposites. *Chem. Mater.* 19:247–53
22. Zhang S, Yu ZJ, Govender T, Luo HY, Li BJ. 2008. A novel supramolecular shape memory material based on partial α-CD-PEG inclusion complex. *Polymer* 49:3205–10
23. Lu XL, Cai W, Zhao LC. 2005. *Pricm 5: Pac. Rim Int. Conf. Adv. Mater. Process., 5th, Pts. 1–5*, pp. 2399–402. Beijing, China: Trans. Tech. Publ.
24. Lu XL, Cai W, Gao ZY, Tang WJ. 2007. Shape memory effects of poly(L-lactide) and its copolymer with poly(ε-caprolactone). *Polym. Bull.* 58:381–91
25. Kim YB, Chung CW, Kim HW, Rhee YH. 2005. Shape memory effect of bacterial poly[(3-hydroxybutyrate)-*co*(3-hydroxyvalerate)]. *Macromol. Rapid Commun.* 26:1070–74
26. Koerner H, Price G, Pearce NA, Alexander M, Vaia RA. 2004. Remotely actuated polymer nanocomposites: stress-recovery of carbon-nanotube-filled thermoplastic elastomers. *Nat. Mater.* 3:115–20
27. Chen GQ, Wu Q. 2005. The application of polyhydroxyalkanoates as tissue engineering materials. *Biomaterials* 26:6565–78
28. Alteheld A, Feng YK, Kelch S, Lendlein A. 2005. Biodegradable, amorphous copolyester-urethane networks having shape-memory properties. *Angew. Chem. Int. Ed.* 44:1188–92
29. Lendlein A, Schmidt AM, Langer R. 2001. AB-polymer networks based on oligo(ε-caprolactone) segments showing shape-memory properties. *Proc. Natl. Acad. Sci. USA* 98:842–47
30. Rousseau IA, Mather PT. 2003. Shape memory effect exhibited by smectic-C liquid crystalline elastomers. *J. Am. Chem. Soc.* 125:15300–1
31. Yakacki CM, Shandas R, Lanning C, Rech B, Eckstein A, Gall K. 2007. Unconstrained recovery characterization of shape-memory polymer networks for cardiovascular applications. *Biomaterials* 28:2255–63
32. Yakacki CM, Willis S, Luders C, Gall K. 2008. Deformation limits in shape-memory polymers. *Adv. Eng. Mater.* 10:112–19
33. Liu GQ, Guan CL, Xia HS, Guo FQ, Ding XB, Peng YX. 2006. Novel shape-memory polymer based on hydrogen bonding. *Macromol. Rapid Commun.* 27:1100–4
34. Jung YC, So HH, Cho JW. 2006. Water-responsive shape memory polyurethane block copolymer modified with polyhedral oligomeric silsesquioxane. *J. Macromol. Sci. B* 45:453–61. Erratum. 45:1189
35. Yakacki CM, Shandas R, Safranski D, Ortega A, Sassaman K, Gall K. 2008. Strong, tailored, biocompatible shape-memory polymer networks. *Adv. Funct. Mater.* 18:1–8

36. Sokolowski WM, Tan SC. 2007. Advanced self-deployable structures for space applications. *J. Spacecr. Rockets* 44:750–54
37. Merline JD, Nair CPR, Ninan KN. 2008. Synthesis, characterization, curing and shape memory properties of epoxy-polyether system. *J. Macromol. Sci. A* 45:312–22
38. Liu C, Chun SB, Mather PT, Zheng L, Haley EH, Coughlin EB. 2002. Chemically cross-linked polycyclooctene: synthesis, characterization, and shape memory behavior. *Macromolecules* 35:9868–74
39. Chung T, Romo-Uribe A, Mather PT. 2008. Two-way reversible shape memory in a semicrystalline network. *Macromolecules* 41:184–92
40. Merline JD, Nair CPR, Gouri C, Shrisudha T, Ninan KN. 2007. Shape memory characterization of polytetra methylene oxide/poly(acrylic acid-coacrylonitrile) complexed gel. *J. Mater. Sci.* 42:5897–902
41. ten Cate AT, Sijbesma RP. 2002. Coils, rods and rings in hydrogen-bonded supramolecular polymers. *Macromolecular Rapid Commun.* 23:1094–112
42. Li JH, Viveros JA, Wrue MH, Anthamatten M. 2007. Shape-memory effects in polymer networks containing reversibly associating side-groups. *Adv. Mater.* 19:2851–55
43. Lendlein A, Jiang HY, Junger O, Langer R. 2005. Light-induced shape-memory polymers. *Nature* 434:879–82
44. Ishida K, Yoshie N. 2008. Two-way conversion between hard and soft properties of semicrystalline crosslinked polymer. *Macromolecules* 41:4753–57
45. Bellin I, Kelch S, Langer R, Lendlein A. 2006. Polymeric triple-shape materials. *Proc. Natl. Acad. Sci. USA* 103:18043–47
46. Weiss RA, Izzo E, Mandelbaum S. 2008. New design of shape memory polymers: mixtures of an elastomeric ionomer and low molar mass fatty acids and their salts. *Macromolecules* 41:2978–80
47. Han SI, Gu BH, Nam KH, Im SJ, Kim SC, Im SS. 2007. Novel copolyester-based ionomer for a shape-memory biodegradable material. *Polymer* 48:1830–34
48. Auad ML, Contos VS, Nutt S, Aranguren MI, Marcovich NE. 2008. Characterization of nanocellulose-reinforced shape memory polyurethanes. *Polym. Int.* 57:651–59
49. Gunes IS, Cao F, Jana SC. 2008. Evaluation of nanoparticulate fillers for development of shape memory polyurethane nanocomposites. *Polymer* 49:2223–34
50. Kim MS, Jun JK, Jeong HM. 2008. Shape memory and physical properties of poly(ethyl methacrylate)/Na-MMT nanocomposites prepared by macroazoinitiator intercalated in Na-MMT. *Compos. Sci. Technol.* 68:1919–26
51. Lee KM, Knight PT, Chung T, Mather PT. 2008. Polycaprolactone-POSS chemical/physical double networks. *Macromolecules* 41:4730–38
52. Hu JL, Ji FL, Wong YW. 2005. Dependency of the shape memory properties of a polyurethane upon thermomechanical cyclic conditions. *Polym. Int.* 54:600–5
53. Morshedian J, Khonakdar HA, Rasouli S. 2005. Modeling of shape memory induction and recovery in heat-shrinkable polymers. *Macromol. Theory Simul.* 14:428–34
54. Tobushi H, Hayashi S, Hoshio K, Ejiri Y. 2008. Shape recovery and irrecoverable strain control in polyurethane shape-memory polymer. *Sci. Technol. Adv. Mater.* 9:015009
55. Gall K, Yakacki CM, Liu YP, Shandas R, Willett N, Anseth KS. 2005. Thermomechanics of the shape memory effect in polymers for biomedical applications. *J. Biomed. Mater. Res. A* 73A:339–48
56. Liu YP, Gall K, Dunn ML, Greenberg AR, Diani J. 2006. Thermomechanics of shape memory polymers: uniaxial experiments and constitutive modeling. *Int. J. Plast.* 22:279–313
57. Khan F, Koo JH, Monk D, Eisbrenner E. 2008. Characterization of shear deformation and strain recovery behavior in shape memory polymers. *Polym. Test.* 27:498–503
58. Qi HJ, Nguyen TD, Castroa F, Yakacki CM, Shandas R. 2008. Finite deformation thermo-mechanical behavior of thermally induced shape memory polymers. *J. Mech. Phys. Solids* 56:1730–51
59. Khonakdar HA, Jafari SH, Rasouli S, Morshedian J, Abedini H. 2007. Investigation and modeling of temperature dependence recovery behavior of shape-memory crosslinked polyethylene. *Macromol. Theory Simul.* 16:43–52
60. Yang B, Huang WM, Li C, Li L. 2006. Effects of moisture on the thermomechanical properties of a polyurethane shape memory polymer. *Polymer* 47:1348–56

61. Lv HB, Leng JS, Liu YJ, Du SY. 2008. Shape-memory polymer in response to solution. *Adv. Eng. Mater.* 10:592–95
62. Chen MC, Tsai HW, Chang Y, Lai WY, Mi FL, et al. 2007. Rapidly self-expandable polymeric stents with a shape-memory property. *Biomacromolecules* 8:2774–80
63. Small W, Buckley PR, Wilson TS, Benett WJ, Hartman J, et al. 2007. Shape memory polymer stent with expandable foam: a new concept for endovascular embolization of fusiform aneurysms. *IEEE Trans. Biomed. Eng.* 54:1157–60
64. Small W, Metzger MF, Wilson TS, Maitland DJ. 2005. Laser-activated shape memory polymer microactuator for thrombus removal following ischemic stroke: preliminary in vitro analysis. *IEEE J. Sel. Top. Quantum Electron.* 11:892–901
65. Small W, Wilson TS, Benett WJ, Loge JM, Maitland DJ. 2005. Laser-activated shape memory polymer intravascular thrombectomy device. *Opt. Expr.* 13:8204–13
66. Yu YL, Ikeda T. 2005. Photodeformable polymers: a new kind of promising smart material for micro- and nano-applications. *Macromol. Chem. Phys.* 206:1705–8
67. Sahoo NG, Jung YC, Goo NS, Cho JW. 2005. Conducting shape memory polyurethane-polypyrrole composites for an electroactive actuator. *Macromol. Mater. Eng.* 290:1049–55
68. Leng JS, Lv HB, Liu YJ, Du SY. 2007. Electroactivate shape-memory polymer filled with nanocarbon particles and short carbon fibers. *Appl. Phys. Lett.* 91:144105
69. Leng JS, Lan X, Liu YJ, Du SY, Huang WM, et al. 2008. Electrical conductivity of thermoresponsive shape-memory polymer with embedded micron sized Ni powder chains. *Appl. Phys. Lett.* 92:014104
70. Hazelton CS, Arzberger SC, Lake MS, Munshi NA. 2007. RF actuation of a thermoset shape memory polymer with embedded magnetoelectroelastic particles. *J. Adv. Mater.* 39:35–39
71. Mohr R, Kratz K, Weigel T, Lucka-Gabor M, Moneke M, Lendlein A. 2006. Initiation of shape-memory effect by inductive heating of magnetic nanoparticles in thermoplastic polymers. *Proc. Natl. Acad. Sci. USA* 103:3540–45
72. Schmidt AM. 2006. Electromagnetic activation of shape memory polymer networks containing magnetic nanoparticles. *Macromol. Rapid Commun.* 27:1168–72
73. Buckley PR, McKinley GH, Wilson TS, Small W, Benett WJ, et al. 2006. Inductively heated shape memory polymer for the magnetic actuation of medical devices. *IEEE Trans. Biomed. Eng.* 53:2075–83
74. Razzaq MY, Anhalt M, Frormann L, Weidenfeller B. 2007. Thermal, electrical and magnetic studies of magnetite filled polyurethane shape memory polymers. *Mater. Sci. Eng. A* 444:227–35
75. Buckley CP, Prisacariu C, Caraculacu A. 2007. Novel triol-crosslinked polyurethanes and their thermorheological characterization as shape-memory materials. *Polymer* 48:1388–96
76. Nguyen TD, Qi HJ, Castro F, Long KN. 2008. A thermoviscoelastic model for amorphous shape memory polymers: incorporating structural and stress relaxation. *J. Mech. Phys. Solids* 56:2792–814
77. Diani J, Liu YP, Gall K. 2006. Finite strain 3D thermoviscoelastic constitutive model for shape memory polymers. *Polym. Eng. Sci.* 46:486–92
78. Chen YC, Lagoudas DC. 2008. A constitutive theory for shape memory polymers. I. Large deformations. *J. Mech. Phys. Solids* 56:1752–65
79. Barot G, Rao IJ. 2006. Constitutive modeling of the mechanics associated with crystallizable shape memory polymers. *Z. Angew. Math. Phys.* 57:652–81
80. Barot G, Rao IJ, Rajagopal KR. 2008. A thermodynamic framework for the modeling of crystallizable shape memory polymers. *Int. J. Eng. Sci.* 46:325–51
81. Kafka V. 2008. Shape memory polymers: a mesoscale model of the internal mechanism leading to the SM phenomena. *Int. J. Plast.* 24:1533–48
82. Chaterji S, Kwon IK, Park K. 2007. Smart polymeric gels: redefining the limits of biomedical devices. *Prog. Polym. Sci.* 32:1083–122
83. Ortega JM, Small W, Wilson TS, Benett WJ, Loge JM, Maitland DJ. 2007. A shape memory polymer dialysis needle adapter for the reduction of hemodynamic stress within arteriovenous grafts. *IEEE Trans. Biomed. Eng.* 54:1722–24
84. Sharp AA, Panchawagh HV, Ortega A, Artale R, Richardson-Burns S, et al. 2006. Toward a self-deploying shape memory polymer neuronal electrode. *J. Neural Eng.* 3:L23–30

85. Small W, Wilson TS, Buckley PR, Benett WJ, Loge JA, et al. 2007. Prototype fabrication and preliminary in vitro testing of a shape memory endovascular thrombectomy device. *IEEE Trans. Biomed. Eng.* 54:1657–66
86. Baer GM, Small W, Wilson TS, Benett WJ, Matthews DL, et al. 2007. Fabrication and in vitro deployment of a laser-activated shape memory polymer vascular stent. *Biomed. Eng. Online* 6:43
87. Sokolowski W, Metcalfe A, Hayashi S, Yahia L, Raymond J. 2007. Medical applications of shape memory polymers. *Biomed. Mater.* 2:S23–27
88. Zheng XT, Zhou SB, Yu XJ, Li XH, Feng B, et al. 2008. Effect of in vitro degradation of poly(D,L-lactide)/β-tricalcium composite on its shape-memory properties. *J. Biomed. Mater. Res. B* 86B:170–80
89. Meng QH, Hu JL. 2008. Study on poly(ε-caprolactone)-based shape memory copolymer fiber prepared by bulk polymerization and melt spinning. *Polym. Adv. Technol.* 19:131–36
90. Vili Y. 2007. Investigating smart textiles based on shape memory materials. *Text. Res. J.* 77:290–300
91. Zhuo HT, Hu JH, Chen SJ, Yeung LP. 2008. Preparation of polyurethane nanofibers by electrospinning. *J. Appl. Polym. Sci.* 109:406–11
92. Xie T, Xiao XC. 2008. Self-peeling reversible dry adhesive system. *Chem. Mater.* 20:2866–68

Annual Review of
Materials Research

Volume 39, 2009

Contents

Materials Advances for Next-Generation Microelectronics

Current Interest

Index

Errata

An online log of corrections to *Annual Review of Materials Research* articles may be found at http://matsci.annualreviews.org/errata.shtml